Cancer Biology
Structural Biology and Molecular Biophysics

A role for JAK2 in mediating cell surface GHR-PRLR interaction

Chen Chen, Jing Jiang, Tejeshwar C. Rao, Tatiana T. Marquez Lago, Stuart J. Frank, André Leier

Department of Genetics, University of Alabama at Birmingham, Birmingham, USA • Division of Endocrinology, Diabetes, and Metabolism, Department of Medicine, University of Alabama at Birmingham, Birmingham, USA • Department of Cell, Developmental, and Integrative Biology, University of Alabama at Birmingham, Birmingham, USA

Reviewed Preprint

Published from the original preprint after peer review and assessment by eLife.

About eLife's process

Reviewed preprint posted
October 26, 2023 (this version)

Posted to bioRxiv
September 5, 2023

Sent for peer review
August 21, 2023

Abstract

Growth hormone (GH) receptor (GHR) and prolactin (PRL) receptor (PRLR) are transmembrane class I cytokine receptors that co-exist in various normal and cancerous cells. Both receptors respond to their associated ligands predominantly by activating the Janus Kinase 2 (JAK2)-signal transducer and activator of transcription (STAT) signaling pathways, and both are also known to initiate receptor-specific JAK2-independent signaling. Together with their cognate ligands, these receptors have been associated with pro-tumorigenic effects in various cancers, including breast cancer (BC). Human GH is known to bind GHR and PRLR, while PRL can only bind PRLR. A growing body of work suggests that GHR and PRLR can form heteromers in BC cells, modulating GH signal transduction. However, the dynamics of PRLR and GHR on the plasma membrane and how these could affect their respective signaling still need to be understood.

To this end, we set out to unravel the spatiotemporal dynamics of GHR and PRLR on the surface of human T47D breast cancer cells and γ2A-JAK2 cells. We applied direct stochastic optical reconstruction microscopy (dSTORM) and quantified the colocalization and availability of both receptors on the plasma membrane at the nanometer scale at different time points following treatment with GH and PRL. In cells co-expressing GHR and PRLR, we surprisingly observed that not only GH but also PRL treatment induces a significant loss of surface GHR. In cells lacking PRLR or expressing a mutant PRLR deficient in JAK2 binding, we observed that GH induces downregulation of membrane-bound GHR, but PRL no longer induces loss of surface GHR. Colocalizations of GHR and PRLR were confirmed by proximity ligation (PL) assay.

Our results suggest that PRLR-GHR interaction, direct or indirect, is indispensable for PRL-but not GH-induced loss of surface GHR and for both GH-induced and PRL-induced increase of surface PRLR, with potential consequences for downstream signaling. Furthermore, our results suggest that JAK2 binding via the receptor intracellular domain's Box1 element is crucial for the observed regulation of one class I cytokine receptor's cell surface availability via ligand-induced activation of another class I cytokine receptor. Our findings shed new light on the reciprocal and collective role that PRLR and GHR play in regulating cell signaling.

eLife assessment

This is an **important** study that characterizes a surprising interaction between two different cytokine/hormone receptors using nanoscale resolution (dSTORM) microscopy. The study provides **solid** evidence that the interaction is ligand-dependent, and is mediated by the receptor-associated intracellular signalling molecule JAK2. While at present limited to growth hormone and prolactin receptors in a limited number of cell lines, there are potentially broad implications for cytokine signalling, as such JAK2-mediated interactions could occur between a range of different cytokines. Moreover, the specific hormone interactions shown in the manuscript may have **important** implications for understanding how these hormones can have differential effects in breast cancer, under different conditions.

Introduction

Growth hormone (GH) and prolactin (PRL) are hormones emanating mainly from the anterior pituitary. The primary function of GH is regulating anabolism and metabolism [1, 2], while PRL has important roles in breast development and lactation [3]. There is mounting evidence pointing at both hormones and their receptors playing roles in various types of cancer [4-11], including breast cancer (BC) [12-17], where GHR is frequently present and PRLR is often found overexpressed [18-25]. While they have been mostly associated with pro-tumorigenic effects, PRL has also been reported to show anti-tumor effects and, like PRLR, has been associated with good prognosis in certain BC subtypes [26-29]. However, a humanized neutralizing monoclonal antibody directed against the extracellular domain of PRLR showed no anti-tumor effect when administered in patients with PRLR-positive metastatic BC [30]. This suggests that PRLRs' pro-tumorigenic function may not be as relevant as previously thought or depends on other circumstances such as the presence or absence of other hormone receptors, with which they may interact.

Both GH receptor (GHR) and PRL receptor (PRLR) are structurally similar transmembrane glycoproteins and belong to the class I cytokine receptor superfamily [31, 32]. GH can bind and introduce a conformational change to both GHR and PRLR, allowing receptor activation and downstream signaling [33-37], but, unlike GH, PRL can only bind to PRLR [36, 38-40]. Both GHR and PRLR lack intrinsic kinase activity. However, as is characteristic of their superfamily members, both receptors contain a proline-rich Box1 motif in the membrane-proximal region of their intracellular domains (ICDs). Following ligand binding, downstream signal transduction involves predominantly activating the associated cytoplasmic tyrosine kinase, Janus kinase 2 (JAK2), bound to the receptors' Box1 elements. This is followed by phosphorylation of the signal transducer and activator of transcription 5 (STAT5) [41, 42], although other receptor-specific JAK2-independent signal transduction pathways may also be activated.

Increasing evidence indicates that GHR and PRLR interact. Two decades ago, it was shown that ovine GHR (oGHR) and PRLR (oPRLR) can tightly associate with each other following stimulation with placental lactogen [43]. These studies utilized chimeric receptors consisting of the extracellular domain (ECD) of human granulocyte and macrophage colony-stimulating factor (hGM-CSF) receptor (hGM-CSFR) along with a part of either oGHR ICD or oPRLR ICD. After hGM-CSF treatment of cells co-expressing oGHR chimera and oPRLR chimera, JAK2 was effectively activated, and protein-protein interaction of both chimeric receptors was detected via co-immunoprecipitation [43, 44]. Additionally, our previous work revealed a specific ligand-independent human GHR (hGHR) - human PRLR (hPRLR) association in human T47D breast cancer

cells, which endogenously express both receptors [45]. Further, the use of split luciferase complementation assays has suggested that hGHR homodimers and hPRLR homodimers form hGHR/hPRLR multimers [46] and extracellular subdomain 2 of the hGHR or hPRLR determines the dimerization partner [47]. Although biochemical studies and luciferase complementation assays strongly support the notion that an interplay between hGHR and hPRLR exists, the observed outcomes are ascribed to total receptors within cells, irrespective of subcellular localization.

In the present study, we directly visualized the cell surface interaction of hGHR and hPRLR and how it changes upon ligand treatment. Specifically, we used direct stochastic optical reconstruction microscopy (dSTORM) [48] to visualize single receptor clusters of hGHR and hPRLR on cell surfaces. In dSTORM, a super-resolution microscopy technique, individual fluorophores cycle through reversible transitions between a dark and a fluorescent state [49]. Thus, a fluorophore emits photons multiple times before permanently being photobleached. These blinking events and their localizations are recorded and, although the exact number of proteins in clusters is difficult to determine, the number of localizations is strongly correlated with the number of receptors [50, 51]. Thus, the dSTORM approach can deliver high-resolution images to reveal the localization or arrangement of individual membrane receptor systems providing valuable insight into their interactions with other proteins at the cell surface. Given that receptors are highly trafficked to and from the cell surface and to avoid signal detection from cytosolic receptors, we used monoclonal antibodies to distinctly label the extracellular S2 domain of GHR and PRLR on non-permeabilized cells. Descriptive spatial analysis using Ripley's K- and L-function [52] indicates that both hGHR and hPRLR are organized in nanometer-scale clusters on the T47D cell surface. To further gain quantitative information about GHR and PRLR nanoclusters, we applied DBSCAN (density-based spatial clustering of applications with noise) [53]. Subsequently, individual cluster contours were delineated, individual clusters were assigned a cluster ID, and receptor abundance was analyzed separately for each cluster and receptor. By doing so, we detected and calculated homomeric and heteromeric hGHR and hPRLR clusters on cell surfaces. Colocalizations of GHR and PRLR were also confirmed by proximity ligation (PL) assay. Lastly, we explored which receptor domains determine the interaction of hGHR and hPRLR by creating different truncated or modified hPRLR variants. Our findings indicate that the intracellular Box1 region is an essential determinant of hGHR and hPRLR association, suggesting JAK2 may play an important role in the observed ligand-induced and PRLR-mediated downregulation of GHR – which could also elicit or add to PRLR's observed anti-tumor effect.

Results

Ligands induce an increase in PRLR localizations and a decrease in GHR localizations at the surface of T47D cells

To investigate the dynamic spatial distribution of endogenous hGHR and hPRLR on the surface of breast cancer cells, we used dSTORM under the total internal reflection fluorescence (TIRF) illumination mode [54]. The dSTORM images show that hGHR and hPRLR form nanometer-scale clusters and are broadly distributed on the surface of T47D cells (**Fig. 1**). To assess the ligands' effects on the spatial distribution of hGHR and hPRLR on the cell surface, we conducted time-course experiments using T47D cells with human GH or human PRL (500 ng/ml each). Such stimulation is known to induce rapid and substantial STAT5 phosphorylation [45]. We first analyzed the cell surface localization density (number of localizations per μm^2) of hGHR or hPRLR in both resting and ligand-stimulated conditions. The abundance of surface-hPRLR was rapidly increased, reaching its maximum after 3 min of GH or PRL treatment with a ~5.6-fold and ~4.5-fold increase compared to the basal value, respectively (**Fig. 2A** and **2B**). This increase was followed by a rapid decline: after GH treatment for 5 min, the localization density dropped from 200.6 ± 14.7 per μm^2 to 57.2 ± 3.6 per μm^2; after PRL treatment for 5 min, the density fell from

159.4 ± 16.2 per μm^2 to 94.8 ± 16.0 per μm^2. In contrast to hPRLR, the density of hGHR significantly decreased from 43.3 ± 5.5 per μm^2 basally to 25.8 ± 2.7 per μm^2 after 3min of GH stimulation. After 5 min and 10 min of GH stimulation, the density of hGHR remained relatively low at 26.6 ± 2.3 per μm^2 and 19.3 ± 1.5 per μm^2, respectively (**Fig. 2C**). Surprisingly, PRL, which does not bind to hGHR, also induced a loss of surface hGHR on T47D cells. After 1 min of PRL treatment, only 36% of hGHR remained on the cell surface compared to the basal state, and hGHR density remained low for at least 10 min (**Fig. 2D**). A schematic illustration of GH- and PRL-induced hGHR and hPRLR density changes is shown in **Fig. 2E**. We previously observed that hGHR and hPRLR specifically co-immunoprecipitate in the absence of added ligands in T47D cells [45]; thus, we postulate that the propensity of hGHR and hPRLR to physically interact underlies our observed loss of hGHR in response to PRL stimulation.

GH or PRL stimulation induces a redistribution of hGHR and hPRLR clusters

We analyzed the dSTORM images using the DBSCAN algorithm to identify different clusters and determine the number of receptor localizations within a cluster (termed 'cluster size') (**Fig. 3A**). We then performed a localization distribution analysis and plotted a histogram of the relative frequency of localizations (termed 'distribution plot' in this study). Representative dSTORM images of hGHR as well as associated distribution plots are shown in **Fig. 3B**.

To gain a better understanding of the changes in GHR-PRLR colocalizations, we obtained and analyzed the corresponding bivariate cluster size distributions. Their median values are summarized in **Fig. 3C** and **3D**. As can be seen, hGHR responds quickly and transiently to GH stimulation by forming larger clusters. After GH treatment for 1 min, the median number of hGHR blinking events in a cluster reaches its peak and amounts to 85.6 ± 20.9 localizations in comparison with 33.3 ± 1.7 localizations per cluster in the basal state (P value = 0.0035). After 5 min, this number is reduced approximately to its pre-stimulation value (29.1 ± 2.2) but appears to continue to fluctuate for at least another 25 minutes (**Fig. 3C**). In turn, hPRLR responds to GH in a less prominent manner: The median number of hPRLR blinking events in a cluster in the basal state is 16.5 ± 0.7. After 3 min of GH stimulation, the median of PRLR cluster size reaches its maximum, which is 22.5 ± 3.9 (P value = 0.1496), and afterward declines to its basal level (**Fig. 3C**).

Like the response to GH, hGHR reacts also quickly to PRL treatment. The median number of hGHR blinking events in a cluster culminates at 1 min of PRL treatment with 45.8 ± 5.0 (compared with basal level, P value = 0.0098). In distinction, hPRLR response to PRL is slower. The median number of hPRLR blinking events in a cluster reaches its peak at 5 min of PRL treatment with a median number of 23.3 ± 2.8 (compared with basal level, P value = 0.0233), and after 10 min the median is only slightly less than that maximum (**Fig. 3D**). Together, these results indicate that upon ligand stimulation hGHR cluster sizes increase transiently and significantly, while changes of hPRLR cluster sizes occur slowly and more subtly.

Spatial proximity of hGHR and hPRLR upon ligand stimulation

Nanoscale interactions of hGHR and hPRLR on the cell surface have yet to be well established. To evaluate the extent of hGHR and hPRLR surface colocalization on T47D cells, we utilized proximity ligation assays (PLAs). In PLAs, a positive signal appears only when two target proteins are in proximity (<40 nm). Notably, individual treatment with GH or PRL for 5 min decreased the PLA signal observed in untreated cells by 34.4% and 28.1%, respectively (**Fig. 4A**), suggesting either ligand caused a reduction in the total number of colocalized hGHR and hPRLR clusters. To further validate these observations, we calculated the ratio of colocalized clusters in dSTORM images. Treatment with GH or PRL for 1 min reduced the proportion of colocalized clusters by nearly 50% (**Fig. 4B** and **4C**). To analyze their compositions, we plotted 3D distributions for the

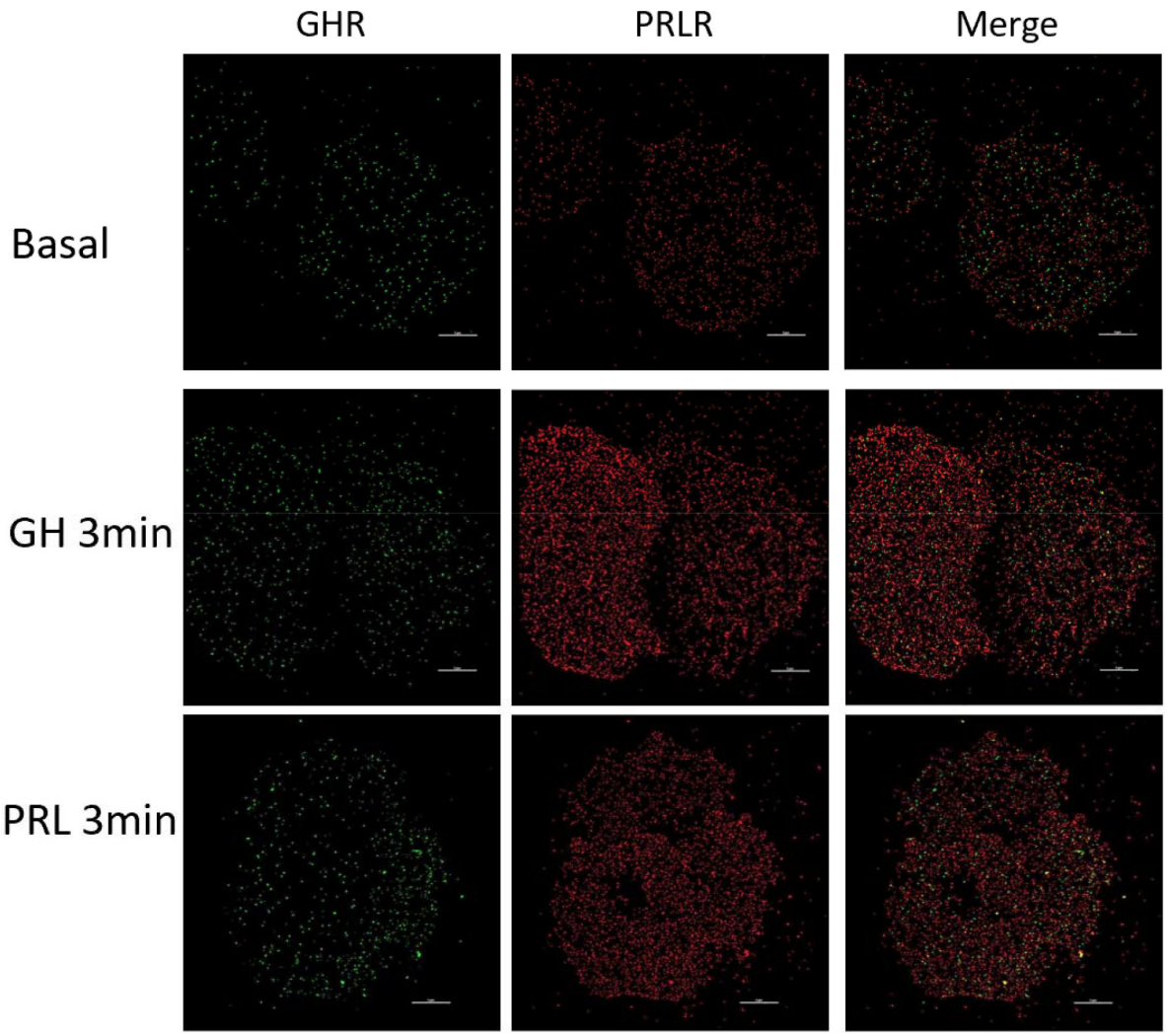

Fig. 1.

Ligand-induced increase of PRLR localizations and decrease of GHR localizations at the surface of T47D cells. A representative set of reconstructed dSTORM images. GHR is labeled with Alexa 568-conjugated antibody (green, channel 1), and PRLR is labeled with Alexa 647-conjugated antibody (red, channel 2). The last column of images shows the merging of these two channels. T47D cells were either left untreated (upper row), exposed to 500ng/mL GH for 3 min (middle row), or exposed to 500ng/mL PRL for 3 min (lower row). Brightness was increased by 40% and Contrast was reduced by 40% to increase visibility. Scale bars 5μm.

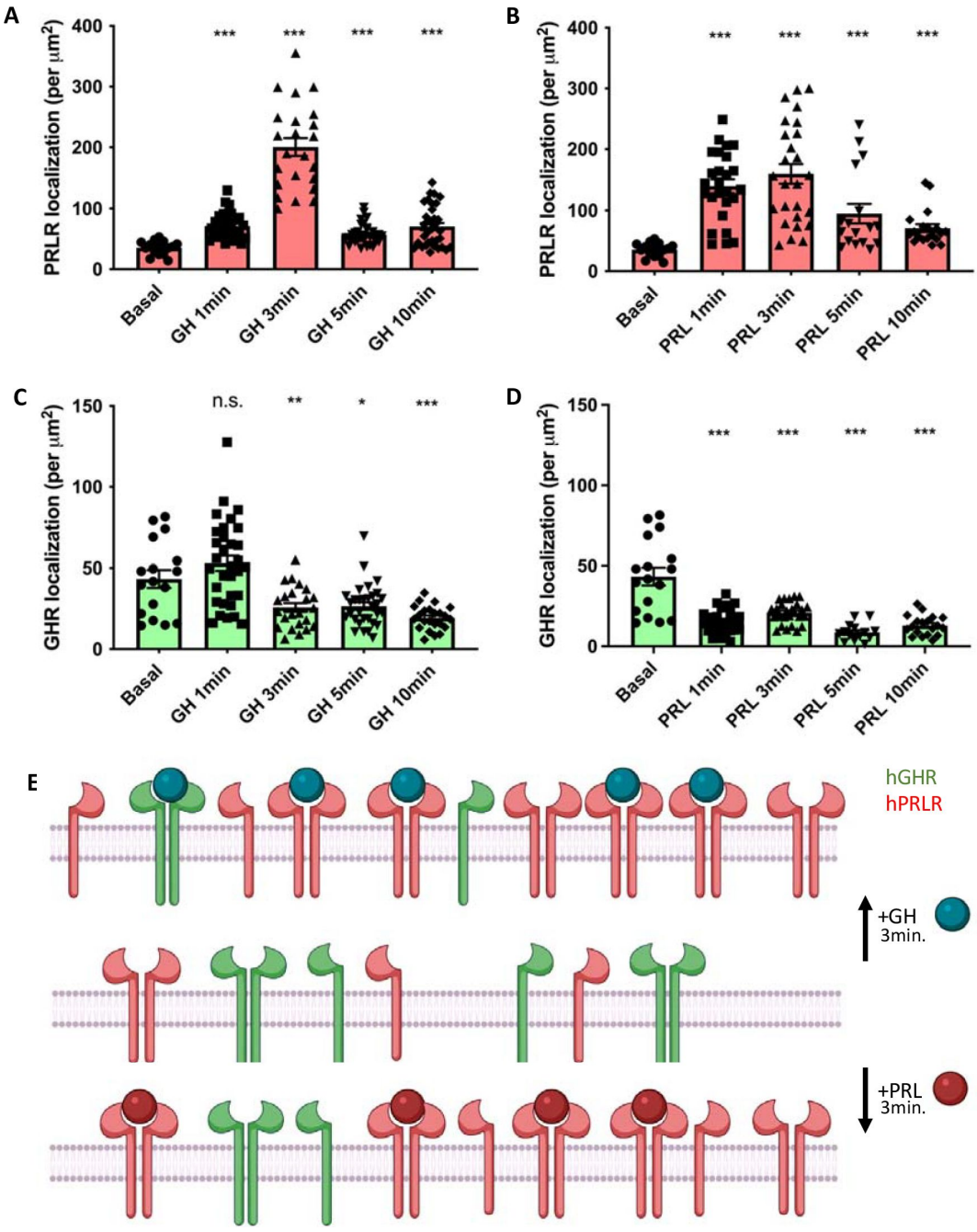

Fig. 2.

(A, B) Quantification of GH-induced (500 ng/ml) (A) and PRL-induced (500 ng/ml) (B) changes of PRLR localizations on the cell surface. **(C, D)** Quantification of GH-induced (C) and PRL-induced (D) changes of GHR localizations on the cell surface. Each data point represents the density of receptors in a 6.25 μm X 6.25 μm area. Data are collected from at least 6 cells from each group and displayed as mean ± SE. * (P<0.05), ** (P<0.01), and *** (P<0.001) indicate the statistical significance in comparison with Basal and are calculated by two-tailed t-tests assuming unequal variances. **(E)** Model depicting hPRLR and hGHR densities and activation schemes in T47D cells.

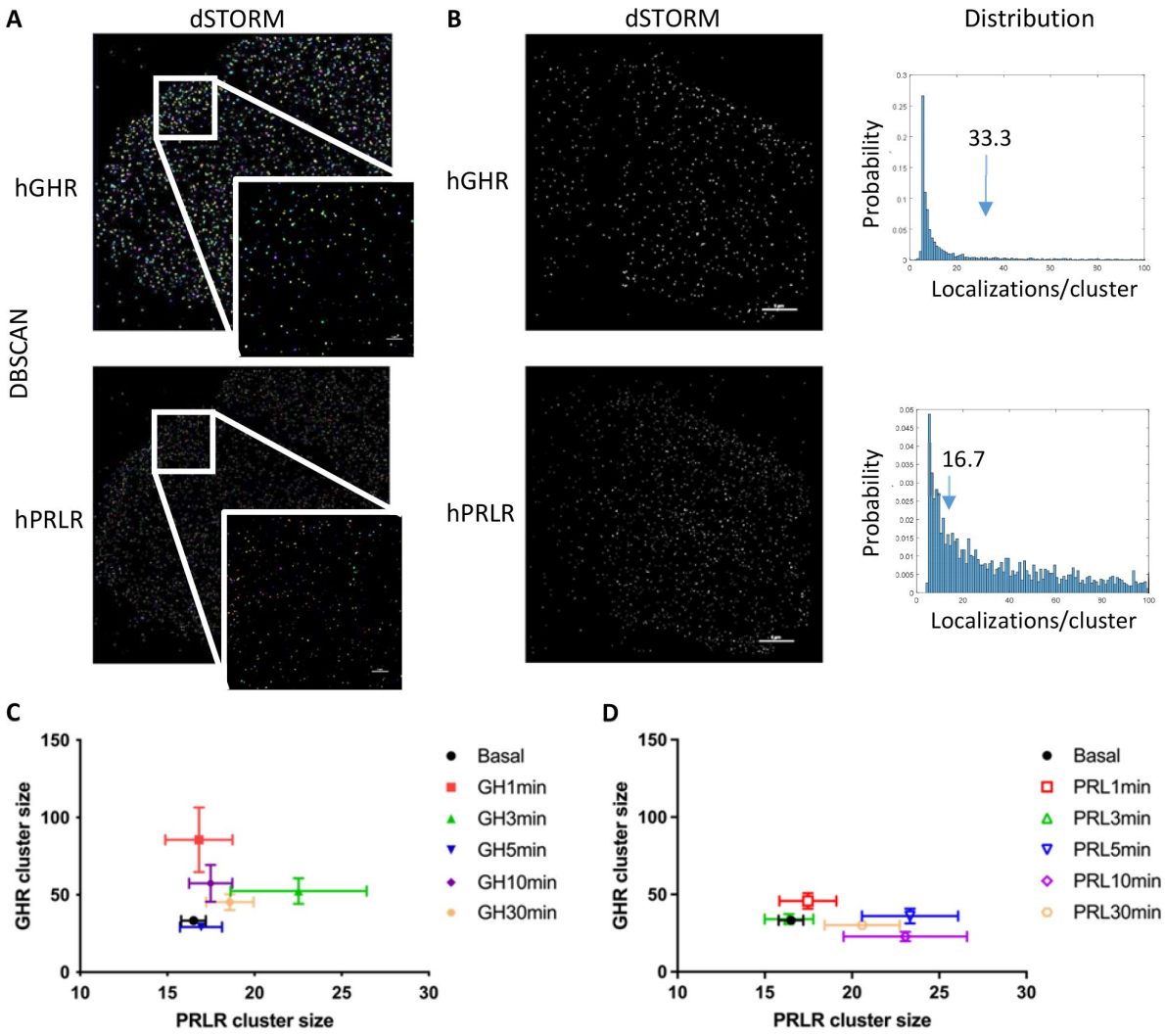

Fig. 3.

GH/PRL stimulation induces a redistribution of hGHR and hPRLR clusters. **(A)** Sample dSTORM images and application of DBSCAN to identify and measure clusters (scale bar, 1 μm). **(B)** Left panels: Representative dSTORM images of hGHR (top) and hPRLR (bottom) on the T47D cell surface in resting state (scale bar, 5 μm). Brightness was increased by 40% for better visibility. Right panels: The corresponding histograms of the relative frequencies of localizations. **(C, D)** The medians of hGHR and hPRLR cluster sizes following GH (C) and PRL (D) treatment are summarized in these plots. The x-axis and y-axis represent hPRLR and hGHR cluster sizes, respectively. Data are collected from at least 6 cells from each group and displayed as median ± SE.

colocalized clusters after ligand treatments (**Fig. S1A** and **S1B**). The probability of observing co-localized clusters with numbers of hGHR and hPRLR that fall into certain bins is identified by color and by the height of the bar on the z-axis. Following GH treatment for 1 min and 3 min, the number of smallest clusters decreased, and the number of medium-sized clusters increased, suggesting a shift of the bivariate distribution of co-localized cluster sizes toward medium-sized clusters (**Fig. S1A**). The distribution of colocalized clusters after 5 min of GH treatment is similar to that at the basal state. In contrast, after treatment with PRL for 3 min or more, the number of medium to large-sized clusters, majoritarily containing either GHR or PRLR, decreased, while the number of smallest clusters increased (**Fig. S1B**). Together, these results demonstrate that hGHR and hPRLR are spatially accessible to each other and form receptor complexes on the T47D cell surface and that the nature of these complexes changes differentially depending on the stimulating ligand.

Reduction of hGHR induced by PRL on the cell surface is dependent on the presence of PRLR

PRL strongly binds PRLR but not GHR. Yet, PRL induces a decrease of hGHR on the surface of cells expressing both hGHR and hPRLR. Thus, we sought to investigate the effect of PRL on hGHR in the absence of hPRLR. We utilized CRISPR/Cas9 technology to generate hPRLR knockout T47D cells (termed $T47D_{\Delta PRLR}$).

In addition, to evaluate isolated hPRLR responses to ligands, we also generated hGHR knockout T47D cells (termed $T47D_{\Delta GHR}$). Immunoblot analysis with specific GHR and PRLR antibodies confirmed the absence of hPRLR in $T47D_{\Delta PRLR}$ cells and hGHR in $T47D_{\Delta GHR}$ cells (**Fig 5A**). Similar to our results with parental T47D cells, GH treatment of $T47D_{\Delta PRLR}$ cells rapidly reduces the density of surface hGHR, suggesting that hPRLR need not be present to allow this GH-induced effect (**Fig 5B**). However, contrary to findings in parental T47D cells, PRL treatment of $T47D_{\Delta PRLR}$ cells fails to modulate hGHR surface density (**Fig 5C**). Like parental T47D cells, treatment of $T47D_{\Delta GHR}$ cells with GH (**Fig 5D**) or PRL (**Fig 5E**) yielded increased hPRLR surface localizations. Thus, we conclude that the PRL-induced decrease of hGHR in T47D cells is dependent on the presence of hPRLR, but the ability of both GH and PRL to increase surface hPRLR in T47D cells is independent of hGHR's presence.

To extend our observations, we next examined the GH and PRL responses in a cellular reconstitution system: γ2A-JAK2 [55-57] is a human JAK2-deficient fibrosarcoma cell line reconstituted with JAK2 that stably expresses JAK2 but lacks hGHR and hPRLR. To independently study the role of each receptor in this setting, we used our previously generated stable transfectants of γ2A-JAK2 cells that harbor either hGHR or hPRLR [58] and verified the presence of the indicated receptor by immunoblotting (**Fig. 5F**). Consistent with the observation in $T47D_{\Delta PRLR}$ cells, γ2A-JAK2-hGHR cells responded with a loss of surface hGHR density to GH stimulation but not to PRL stimulation (**Fig. 5G**). Interestingly, as in $T47D_{\Delta GHR}$ cells, treatment of γ2A-JAK2-hPRLR cells with either GH or PRL (**Fig. 5H**) promotes increased surface hPRLR. Thus, our findings in both cell systems suggest that hPRLR-hGHR interaction, direct or indirect, is indispensable for PRL-induced but not for GH-induced loss of surface hGHR.

Box 1 region in hPRLR contributes to PRL-induced GHR downregulation

The hPRLR-dependent PRL-induced hGHR downregulation indicates that hPRLR can modulate the density of hGHR on the cell surface in response to PRL. To investigate this interaction, we generated a set of truncation or deletion mutants of hPRLR: (1) hPRLR-tr292, which truncates the intracellular domain of hPRLR distal to the membrane-proximal intracellular domain box 1 element; (2) hPRLR-tr238, which contains only 4 amino acids of the proximal intracellular domain

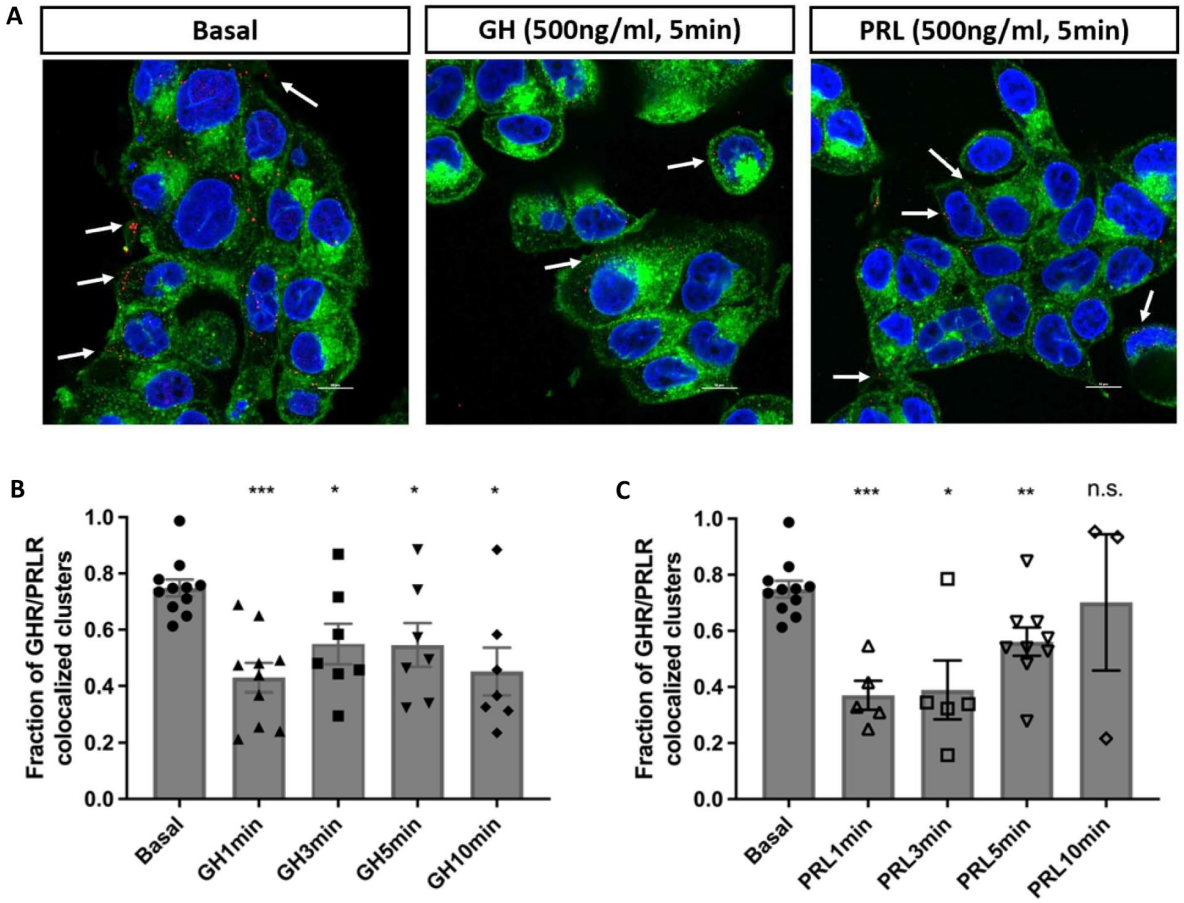

Fig. 4.

Spatial proximity of hGHR and hPRLR upon ligand stimulation. **(A)** Proximity ligation assays were performed in T47D cells (scale bar, 10 μm). Here we show representative confocal microscopy images of T47D cells at resting and ligand stimulation conditions. The PLA signal (red dots) corresponds to hGHR and hPRLR complexes, wheat germ agglutinin (green staining) corresponds to the cell membrane, and DAPI (blue staining) corresponds to cell nuclei. **(B, C)** hGHR and hPRLR colocalization changes in T47D cell surface following 500 ng/ml GH (B) or PRL (C) treatment. Each data point represents a ratio of clusters, which contain both hGHR and hPRLR, to the total clusters on the cell surface. Data are displayed as mean± SE. * ($P<0.05$), ** ($P<0.01$), and *** ($P<0.001$) indicate the statistical significance in comparison with Basal and are calculated by a two-tailed t-test assuming unequal variance.

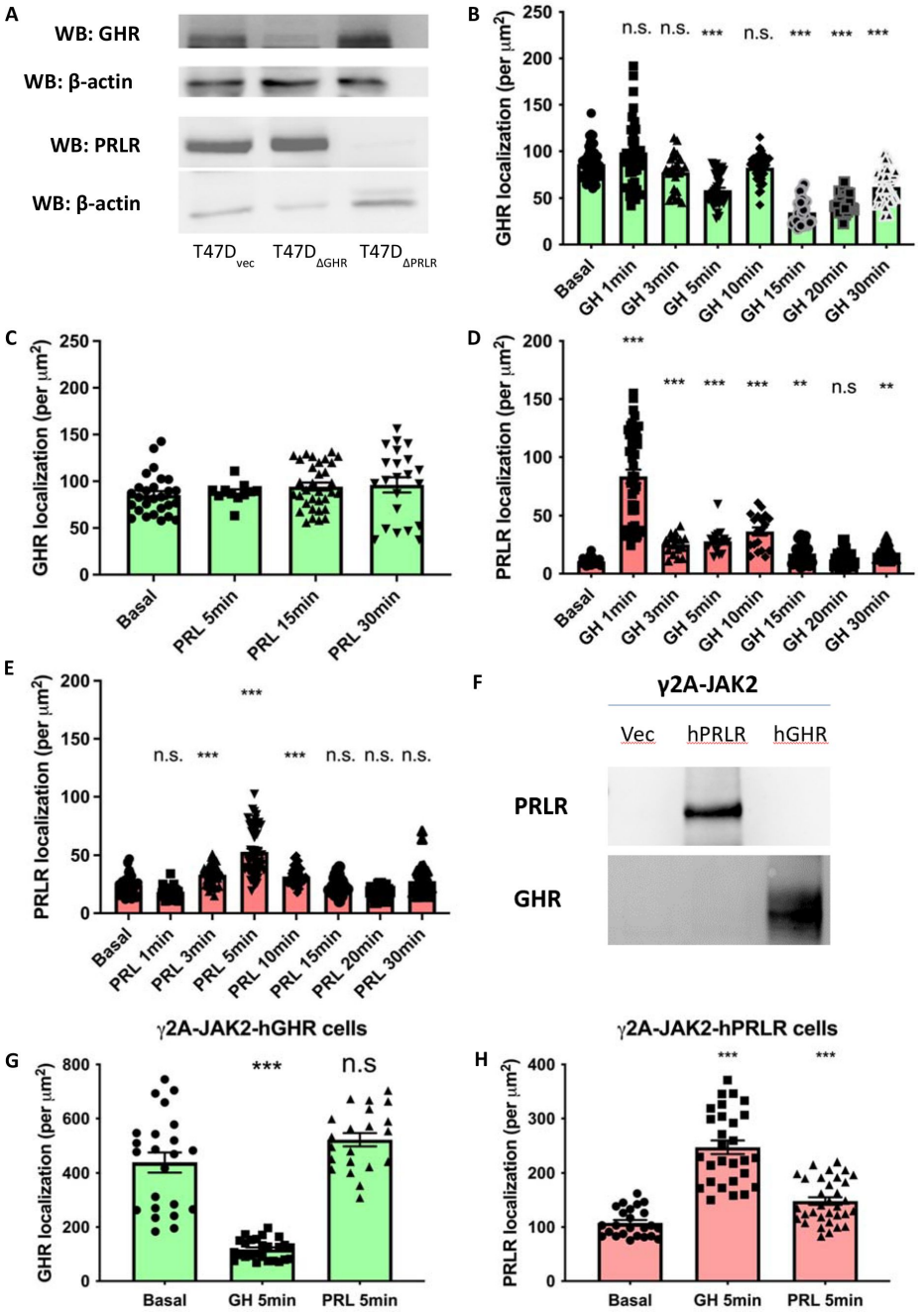

Fig. 5.

PRL-induced reduction of hGHR on the cell surface depends on the presence of PRLR. **(A)** Detergent cell extracts of T47D$_{vec}$, T47D$_{\Delta GHR}$, and T47D$_{\Delta PRLR}$ were analyzed by immunoblotting with anti-GHR$_{cyt\text{-}AL47}$, anti-PRLR$_{cyt,}$ and anti-β-actin antibodies. **(B)** In T47D$_{\Delta PRLR}$, GH (500 ng/ml) induces downregulation of hGHR localizations on the cell surface, while **(C)** PRL does not change hGHR localizations. **(D, E)** In T47D$_{\Delta GHR}$ cells, GH (D) and PRL (E) incite an increase of hPRLR on the cell surface. Data are displayed as mean ± SE. * (P<0.05), ** (P<0.01), and *** (P<0.001) indicate the statistical significance in comparison with Basal and are calculated by a two-tailed t-test assuming unequal variance. **(F)** γ2A-JAK2 cells with stable expression of hGHR or hPRLR. Detergent extracts were resolved by SDS-PAGE and immunoblotted with anti-GHR$_{cyt\text{-}\ AL47}$ and anti-PRLR$_{cyt\text{-}AL84}$ antibodies. **(G, H)** Serum-starved γ2A-JAK2-hGHR cells (G) or γ2A-JAK2-hPRLR cells (H) were treated with GH (500 ng/ml) or PRL (500 ng/ml) for 5 min. Localizations of hGHR in γ2A-JAK2-hGHR cells were decreased after GH treatment while remaining the same after PRL treatment compared to the basal state. Localizations of hPRLR in γ2A-JAK2-hPRLR cells were increased by GH or PRL treatment. Data are displayed as mean ± SE. * (P<0.05), ** (P<0.01), and *** (P<0.001) denote the statistical significance in comparison with Basal and are calculated by a two-tailed t-test assuming unequal variance.

and does not include box 1; and (3) hPRLR-Δbox1, in which the box 1 region (243aa-251aa) is internally deleted (shown in **Fig. 6A**). Expression of hPRLR-tr292, hPRLR-tr238, and hPRLR-Δbox1, as well as wild-type hPRLR, was detected by immunoblotting using monoclonal antibodies targeting the ECD of PRLR ($mAb_{ext\text{-}1.48}$). Since hPRLR-tr238 contains only 4aa in its ICD, no immunoblot signal was detected using a polyclonal antibody ($Ab_{AL\text{-}84}$) targeting the hPRLR ICD. In contrast, the expression of hPRLR-tr292 was easily detected by $Ab_{AL\text{-}84}$ (**Fig. 6B**). We then transiently transfected each hPRLR construct into the γ2A-JAK2-hGHR cells, which stably express hGHR, and analyzed the changes of cell surface hGHR localizations. In cells expressing wild-type hPRLR (hPRLR-WT), the localizations of hGHR significantly decreased 3 min post-exposure to GH and PRL (**Fig. 6C**). Similarly, under the same treatment, in cells expressing hPRLR-tr292, the localization of hGHR on the cell membrane was reduced in response to each ligand (**Fig. 6D**). However, in hPRLR-tr238-expressing cells, the localization of hGHR was diminished by GH stimulation but slightly increased by PRL stimulation (**Fig. 6E**). To further investigate the role of the box1 region for hGHR and hPRLR functional interaction, we studied hPRLR-Δbox1 expressing cells and found that upon PRL treatment, hGHR localizations did not decrease on the cell surface (**Fig. 6F**). As a negative control, we transfected the cells with vector (pcDNA3.1). hGHR localization decreased upon GH stimulation but remained at basal levels upon PRL stimulation (**Fig. 6G**). In addition, in hPRLR-ΔBox1 and hGHR expressing cells, the JAK2 and STAT5 tyrosine phosphorylation levels were assessed in response to GH and PRL stimulations. Treatment of 500ng/ml GH induces a dramatic increase in both JAK2 and STAT5 phosphorylation. In contrast, 500ng/ml PRL treatment does not cause JAK2 or STAT5 phosphorylation (**Fig. 6H**), consistent with PRLR Box1 being required for effective coupling of PRL occupancy of PRLR to activation of JAK2 and phosphorylation of STAT5 and the inability of PRL to signal via GHR.

Next, we analyzed colocalization in each group. In the resting state, the ratios of GHR-PRLR-colocalization clusters are relatively higher in hPRLR-WT- and hPRLR-tr292-expressing cells in comparison with hPRLR-tr238- and hPRLR-ΔBox1-expressing cells (**Fig. 6I**). This suggests that the box 1 region in hPRLR plays a critical role in stabilizing the hGHR-hPRLR complexes in the basal state.

Box 1 region in hGHR plays an essential role in regulating PRLR and GHR interaction

From our observations (**Fig. 6**), we concluded that the JAK2 binding site, i.e., the box 1 region, in hPRLR is required for PRL-induced hGHR down-regulation from the cell surface. To further assess whether the JAK2 binding site on hGHR is also essential, we generated hGHR-ΔBox1, in which the box 1 region (297aa – 305aa) was deleted (**Fig. 7A**). In cells expressing both hGHR-ΔBox1 and hPRLR we observed that GH does not alter the hGHR-ΔBox1 localizations on the cell surface, while PRL slightly increases hGHR-ΔBox1 localizations (**Fig. 7B**). Together, these results re-affirm that binding of JAK2 to hGHR is also required for hPRLR-mediated regulation of hGHR availability on the cell surface.

Materials and Methods

Materials

Common reagents were purchased from Sigma Aldrich Corp. (St. Louis, MO) unless otherwise noted. Fetal bovine serum was purchased from Atlanta Biologicals (Lawrenceville, GA). Cell culture medium, penicillin/streptomycin and trypsin were purchased from Corning (Corning, NY). Recombinant hGH was kindly provided by Eli Lilly & Co. (Indianapolis, IN). Recombinant human PRL was obtained from the National Hormone and Pituitary Program.

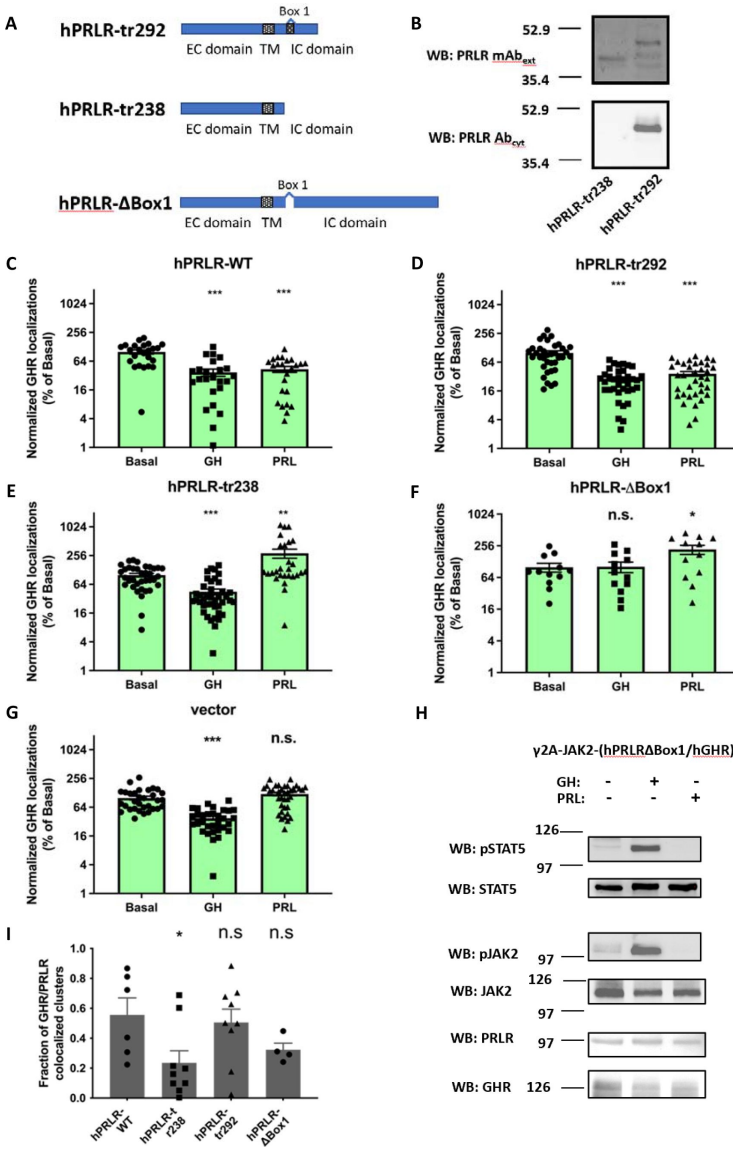

Fig. 6.

Box 1 region in hPRLR contributes to PRLR-induced GHR downregulation. **(A)** Diagrams of employed mutant hPRLR variants with truncations or deletion in the intracellular domain. ECD, extracellular domain; TMD, transmembrane domain; ICD, intracellular domain. **(B)** γ2A-JAK2-hGHR cells were transiently transfected with hPRLR-tr292 and hPRLR-tr238. Cell extracts were resolved by SDS-PAGE and blotted with anti-PRLR $mAb_{ext\text{-}1.48}$ and anti-$PRLR_{cyt\text{-}AL84}$. **(C-G)** γ2A-JAK2-hGHR cells were transfected with (C) wild-type hPRLR (hPRLR-WT), (D) hPRLR truncated at 292 aa (hPRLR-tr292), (E) hPRLR truncated at 238 aa (hPRLR-tr238), (F) hPRLR with box1 motif deleted (hPRLR-ΔBox1) and (G) vector pcDNA3.1 (vector). Transfected cells were imaged by dSTORM microscopy and analyzed using the DBSCAN algorithm. The density of hGHR localizations on the cell surface was calculated. Each data point represents the density of hGHR in a cell surface area of size 6.25 μm X 6.25 μm. Data are collected from at least 6 cells (4 ROIs per cell) from each group, and values are displayed as mean ± SE (from three independent experiments). Data are normalized such that the basal is 100%. * (P<0.05), ** (P<0.01), and *** (P<0.001) denote the statistical significance in comparison with Basal and are calculated by a two-tailed t-test assuming unequal variance. **(H)** Detergent cell extracts of hPRLR-ΔBox1 and hGHR-expressing cells were analyzed by immunoblotting. After 5 hrs. starvation, cells were treated with GH (500 ng/ml) or PRL (500 ng/ml) for 10 min. In each experiment, the average Basal value is considered 100%. **(I)** Fraction of GHR/PRLR colocalized clusters. In the resting state, the colocalization ratio is significantly lower for cells expressing hPRLR-tr238 than for those expressing hPRLR-WT. Each data point represents the ratio of the number of clusters, which contain both hGHR and hPRLR, to the total number of clusters on the cell surface. Data are displayed as mean ± SE. * (P<0.05) indicates statistical significance in comparison with WT and is calculated by a two-tailed t-test assuming unequal variance (all bars without an asterisk are not significant).

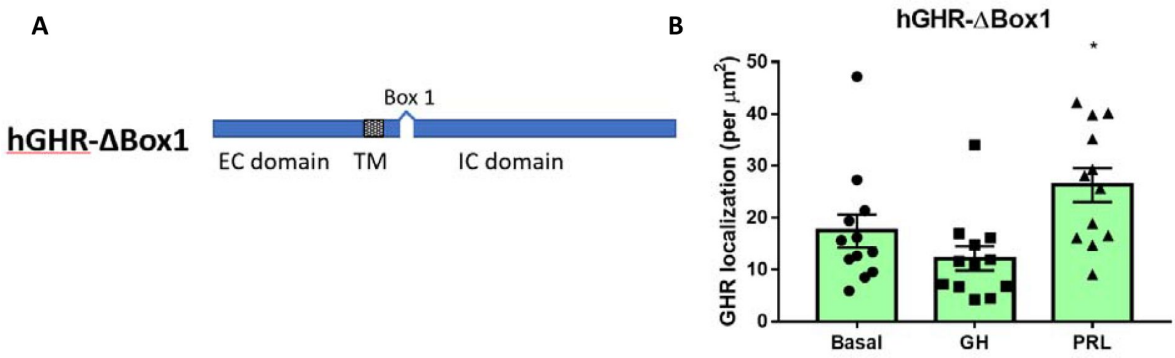

Fig. 7.

Box 1 region in hGHR also plays an important role in PRLR and GHR interaction. **(A)** Diagram of hGHR-ΔBox1 showing the deleted box 1 region in the intracellular domain of hGHR. **(B)** γ2A-JAK2-hPRLR cells were transfected with hGHR-ΔBox1. Transfected cells were imaged by dSTORM microscopy and analyzed using DBSCAN. The density of hGHR localizations on the cell surface was calculated. Each data point represents the density of hGHR in a cell surface area of size 6.25 μm X 6.25 μm. Data are collected from at least 6 cells for each group and displayed as mean ± SE. * (P<0.05), ** (P<0.01), and ***(P<0.001) indicate the statistical significance in comparison with Basal and are calculated by a two-tailed t-test assuming unequal variance.

Antibodies

Polyclonal anti-$GHR_{cytAL-47}$ (1:1000) against the intracellular domain of GHR described previously [59] was used as the primary antibody for western blot analysis. Monoclonal anti-$GHR_{ext-mAb}$ (1:1000) against the extracellular S2 domain of GHR [60] and monoclonal anti-$PRLR_{ext-mAb}$ against the extracellular S2 domain of human PRLR [47] was used for microscopy. A detailed description is provided in the references. The following secondary antibodies were used: Alexa Fluor 568 goat anti-mouse IgG1 (Invitrogen #A-21124) (1:1000), Alexa Fluor 647 goat anti-mouse IgG2b (Invitrogen #A-21242) (1:1000), Alexa Fluor 647 goat anti-mouse IgG1 (Invitrogen #A-21240) (1:1000) and Alexa Fluor 568 goat anti-mouse IgG2b (Invitrogen # A-21144) (1:1000).

Cloning and constructs

The human GHR cDNA in pcDNA1 was a generous gift from R. Ross (University of Sheffield, Sheffield, UK). The human PRLR cDNA in pEF/V5/HIS was generously provided by C. Clevenger (Virginia Commonwealth University, Richmond, VA). hPRLR-tr238 and hPRLR-tr292 were generated by amplifying with external primers containing EcorI site and a stop codon with XhoI site after the sequence of 238 or 292 amino acid, respectively. hPRLR-ΔBox1, and hGHR-Δbox1 were generated by overlap extension polymerase chain reaction (PCR) with associated primers and cloned into pcDNA3.1(+) vector.

Cell culture and transfections

Human T47D breast cancer cells were purchased from American Type Culture Collection (Manassas, VA). Cells were maintained in RPMI 1640 medium supplemented with 10% fetal bovine serum (FBS), 100 units/ml penicillin and 100 µg/ml streptomycin in a humidified atmosphere of 5% CO2 and 95% air at 37 °C.

γ2A-JAK2 cells were generated by transfection of γ2A cells [55] with pcDNA3.1(+)/zeo-JAK2 and maintained in culture, as described previously [56, 57]. The generation of γ2A-JAK2-GHR and γ2A-JAK2-PRLR cells has been previously described [58].

Transient expression of receptors was achieved by using Lipofectamine LTX Plus (Invitrogen), transfecting 0.3 pmol plasmid DNA per 6-cm^2 dish.

Western blot

Cells were serum starved for 5 hours and treated with 500 ng/ml GH or 500 ng/ml PRL at 37 °C for 10 min. Stimulations were terminated by washing the cells with ice-cold phosphate-buffered saline supplemented with 0.4 mM sodium orthovanadate. Cells were lysed in lysis buffer for 30 min at 4°C. Then cell lysates were centrifuged at 15,000 g for 10 min at 4°C. The protein extracts (supernatant) along with SDS sample buffer were resolved by SDS-PAGE.

Sample preparation for imaging

Cells were seeded into either eight well #1.5 coverslip bottom dishes (Ibidi) or 25 mm #1.5 coverslips (Electron Microscopy Sciences). Cells were serum starved for 5 hours, then treated with GH (500 ng/ml), PRL (500 ng/ml) at 37 °C for the indicated time. Then the cells were washed with PBS three times and fixed with 4% PFA (paraformaldehyde) for 10 min. After multiple washes with PBS, cells were blocked with 5% normal horse serum, 5% normal goat serum, 1% BSA for 30 min. Lastly, cells were incubated in primary antibody for 3h and secondary antibody for 70 min at 37°C.

dSTORM imaging and data analysis

dSTORM experiments were conducted on an inverted Nikon Ti2 N-STORM microscope equipped with a 100 X 1.49 NA oil immersion objective (Nikon, Japan), 488 and 647 nm lasers, and an iXon DU-897 ultra EMCCD camera (Andor, Oxford Instruments). The dSTORM imaging buffer included

glucose oxidase (Sigma, St Louis, Missouri), glucose (Sigma, St Louis, Missouri), catalase (Roche, Penzberg, Germany), and β-mercaptoethanol (Sigma, St Louis, Missouri). The cell membrane was focused using TIRF excitation, which selectively images within 100-150 nm of the cell membrane, making it an excellent method to study surface distribution of membrane proteins. For dual color STORM imaging, the sample was illuminated with 561nm or 647 nm lasers alternatively and 40,000 frames of images were acquired per channel. The chromatic offset associated with the different acquisition wavelengths was corrected using 0.1 μm microspheres [61, 62].

dSTORM images were reconstructed using the built-in STORM module in NIS-Elements (Nikon). The localizations list was exported and further analyzed in *Matlab*. In particular, for the DBSCAN cluster analysis, we employed Clus-DoC directly on the list of localizations, utilizing the parameters of a minimum of 4 neighbors within a cluster radius of 20nm [63].

Statistical analysis

Imaging and biochemical experiments were carried out at least three times to ensure reproducibility. Data were analyzed using unpaired, two-tailed t-tests. *Prism* software was used for statistical analysis (GraphPad Inc, USA). Data are presented as means ± s.e.m.

Discussion

The non-ligand-bound states of hGHR and hPRLR have been extensively investigated. Pre-homodimerization of hGHR and hPRLR has been reported using structural and biochemical methods [35, 64-67]. At the same time, a recent study supports the notion that GHR, at physiological densities, exists as monomers on the cell surface and becomes activated by a ligand-induced dimerization [68]. The current study uses a highly precise and sensitive single-molecule localization microscopy approach to study the formation of hGHR and hPRLR nanoclusters and the cell surface receptor availability. Our super-resolution images reveal that in human T47D breast cancer cells and the γ2A-JAK2 cell exogenous expression system, the cluster size of hGHR and hPRLR in the basal state range from a few localizations per cluster up to a thousand localizations per cluster.

With GH or PRL treatment, the number of hGHR on both T47D and γ2A-JAK2 cell surfaces is decreased, indicating the removal of surface hGHR. Moreover, the distribution curve of hGHR shifts toward larger cluster sizes (**Fig. 3**), suggesting a ligand-induced aggregation of receptors. In turn, hPRLR numbers dramatically increase on the cell surface in response to ligand stimulation. The newly presented hPRLR clusters may impact the distribution of cluster sizes, which may explain why the median of hPRLR cluster sizes does not change much with ligand treatment.

Our PL assay data indicate that distances between hGHR and hPRLR are small (less than 40nm). This implies that hGHR and hPRLR form co-localized clusters in unstimulated states, suggesting hGHR and hPRLR are physically accessible to one other. With GH stimulation, the fraction of co-localized receptors is decreased. Given that GH treatment enhances the coimmunoprecipitation of total cellular hGHR and hPRLR [45], the decrease in co-localized surface receptors can likely be attributed to removing co-localized receptors from the cell surface.

It is well documented that hPRLR is engaged by both PRL and GH, while hGHR only responds to GH [36, 38, 39]. Unexpectedly, we found that PRL induces a down-regulation of cell surface hGHR in cells that co-express hGHR and hPRLR (**Fig. 2**), indicating that hPRLR directly or indirectly interacts with hGHR. Interestingly, PRL was unable to induce hGHR down-regulation in cells either lacking hPRLR or expressing hPRLR without its Box1 region (hPRLR-tr238 or hPRLR-ΔBox1), suggesting that JAK2 and PRLR association is required for hGHR-hPRLR interaction that in

turn allows PRL-induced hGHR downregulation. Notably, previous work showed that GHR and JAK2 association is necessary for JAK2 to stabilize cell surface GHR and inhibit constitutive GHR down-regulation [57]. Furthermore, single-particle tracking studies showed that, in the presence of JAK2, a higher level of ligand-induced dimerization of GHR was observed [68].

Moreover, JAK2 with intact kinase activity is required for GH-induced GHR down-regulation [57]. Similarly, the box1 region of PRLR also associates with JAK2, and deletion or modulation of the last proline residue of box1 abrogates PRLR function [69]. Collectively, these findings suggest that the box1 regions in hGHR and hPRLR play a crucial role in the transduction of the individual signaling cascades and hGHR-hPRLR association.

Here we found that, in the resting state, the degree of hGHR-hPRLR colocalization is higher in cells expressing hPRLR with the box1 motif. This suggests JAK2 may not only stabilize GHR but also support the formation of hGHR-hPRLR-containing clusters. Previously, it has been suggested that such clusters are comprised of hGHR homodimers and hPRLR homodimers that together form (hGHR-hGHR) – (hPRLR-hPRLR) hetero-multimers or higher order oligomers [46]. Indeed, because the intracellular domains (ICD) of both hGHR and hPRLR are highly disordered, the flexibility of their ICDs may provide room for recruiting JAK2 and stabilizing the hGHR-hPRLR association [70, 71]. Moreover, a study of the crystal structure of erythropoietin receptor (EPOR) and leptin receptor (LEPR), which also belong to the class I cytokine receptor family, revealed recently that JAK2/EPOR and JAK2/LEPR complexes contained four JAK2 and four EPOR or LEPR molecules, respectively [72]. Hence, it is possible that hGHR-hGHR homodimers and hPRLR-hPRLR homodimers form complexes in a similar fashion (**Fig. 8**). We propose that this JAK2/Box1-mediated interaction of receptors is not limited to hGHR and hPRLR but may generalize to other receptors of the class I cytokine receptor family. We note, however, that determinants within particular receptors (perhaps residing in their extracellular and/or transmembrane domains) and their intracellular JAK2 association domains may facilitate, to varying degrees, their propensity to form multimeric aggregates. GHR and PRLR, for example, may tend to do so more avidly with each other than either one does with other cytokine receptors. Additional studies are required to determine and understand the modes and functions of the hGHR-hPRLR association.

Lastly, hPRL/hPRLR-mediated downregulation of surface hGHR may be a relevant factor in the observed anti-tumor effect of PRLR signaling, especially in triple-negative breast cancer (TNBC) expressing PRLR but lacking other interfering hormone receptors. As previously shown, the TNBC cell lines MDA-MB-231 and MDA-MB-453 show significantly increased GHR [15] while expressing no or only endogenous levels of PRLR, respectively [28]. PRL treatment significantly decreased cell viability and invasive capacity of MDA-MB-231 cells following the restoration of PRLR expression. In MDA-MB-453 cells, PRL caused a significant reduction in cell viability. A xenograft model with inoculated MDA-MB-453 cells confirmed the growth inhibitory effect of PRL treatment *in vivo*, suggesting PRLR expression as an indicator of a favorable prognosis. Future research will have to investigate our hypothesis that PRLR-mediated downregulation of surface GHR contributed to the anti-tumoral effect of PRL treatment in PRLR-positive TNBC.

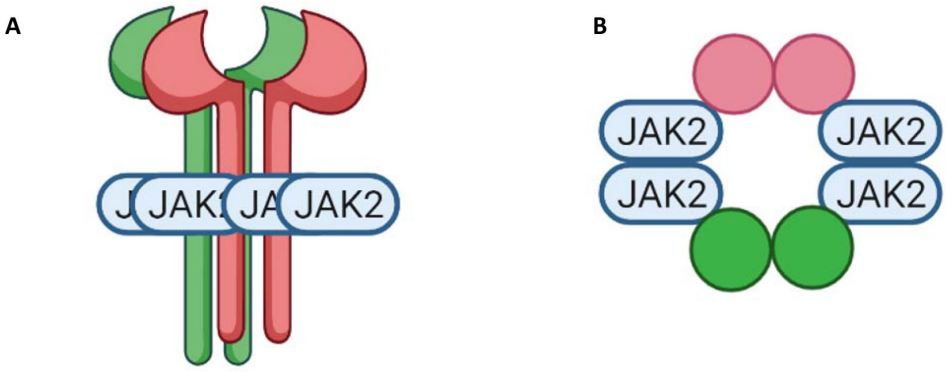

Fig. 8.

Model of JAK2 stabilizing GHR-GHR and PRLR-PRLR heteromers. **(A)** Schematic representation of GHRs homodimer and PRLRs homodimer form a heteromer, which contains two PRLRs (red), two GHRs(green), and four JAK2(blue). **(B)** A top view of the JAK2/PRLR/GHR multimer.

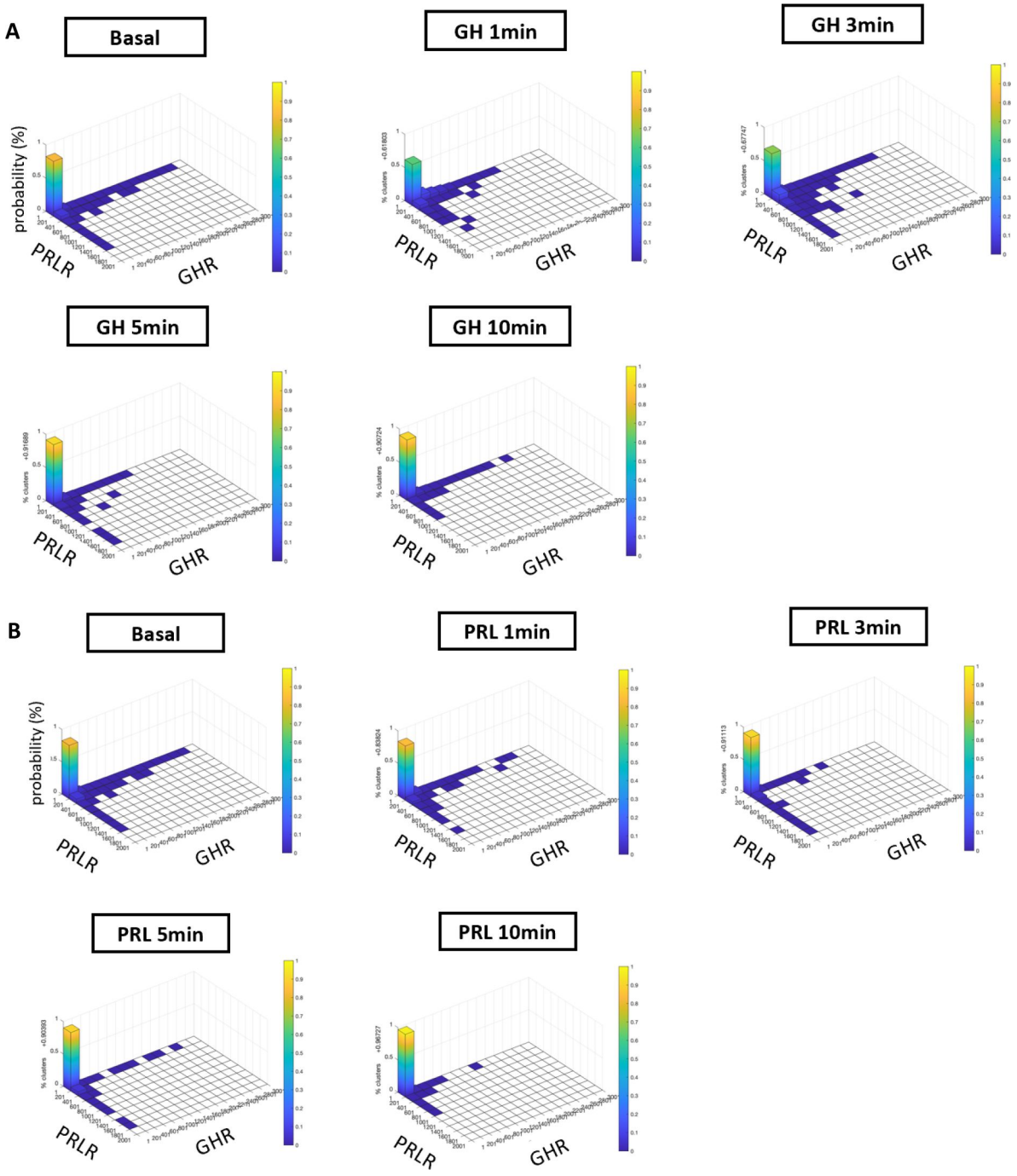

Fig. S1

The size distributions of co-localized clusters are shown in 3D plots, where the binned x-axis represents the number of hGHR localizations, the binned y-axis represents the number of hPRLR localizations, and the z-axis represents the probability of the cluster. Each bin has a size of 200 localizations. Both GH **(A)** and PRL **(B)** induce a distinct change in the composition of co-localized clusters.

References

1. Isaksson O.G., Eden S., Jansson J.O. (1985) **Mode of action of pituitary growth hormone on target cells** *Annu Rev Physiol* **47**:483–99

2. Moller N., Jorgensen J.O. (2009) **Effects of growth hormone on glucose, lipid, and protein metabolism in human subjects** *Endocr Rev* **30**:152–77

3. Brooks C.L. (2012) **Molecular mechanisms of prolactin and its receptor** *Endocr Rev* **33**:504–25

4. Gonzalez-Lucano L.R., et al. (2012) **Increased expression of the prolactin receptor is associated with malignant laryngeal tumors** *Exp Ther Med* **3**:603–607

5. Ascencio-Cedillo R., et al. (2015) **Prolactin and prolactin receptor expression in cervical intraepithelial neoplasia and cancer** *Pathol Oncol Res* **21**:241–6

6. Harris J., et al. (2004) **Prolactin and the prolactin receptor: new targets of an old hormone** *Ann Med* **36**:414–25

7. Asad A.S., et al. (2020) **The role of the prolactin receptor pathway in the pathogenesis of glioblastoma: what do we know so far?** *Expert Opin Ther Targets* **24**:1121–1133

8. Sethi B.K., Chanukya G.V., Nagesh V.S. (2012) **Prolactin and cancer: Has the orphan finally found a home?** *Indian J Endocrinol Metab* **16**:S195–8

9. Boguszewski C.L., Boguszewski M. (2019) **Growth Hormone's Links to Cancer** *Endocr Rev* **40**:558–574

10. Strous G.J., et al. (2020) **Growth Hormone Receptor Regulation in Cancer and Chronic Diseases** *Front Endocrinol (Lausanne)* **11**

11. Chhabra Y., Waters M.J., Brooks A.J. (2011) **Role of the growth hormone-IGF-1 axis in cancer** *Expert Rev Endocrinol Metab* **6**:71–84

12. Clevenger C.V., Rui H. (2022) **Breast Cancer and Prolactin - New Mechanisms and Models** *Endocrinology* **163**

13. Shemanko C.S. (2016) **Prolactin receptor in breast cancer: marker for metastatic risk** *J Mol Endocrinol* **57**:R153–R165

14. Goffin V. (2017) **Prolactin receptor targeting in breast and prostate cancers: New insights into an old challenge** *Pharmacol Ther* **179**:111–126

15. Zhu X., et al. (2020) **Growth hormone receptor promotes breast cancer progression via the BRAF/MEK/ERK signaling pathway** *FEBS Open Bio* **10**:1013–1020

16. Subramani R., et al. (2017) **Role of Growth Hormone in Breast Cancer** *Endocrinology* **158**:1543–1555

17. Xu J., et al. (2013) **The role of prolactin receptor in GH signaling in breast cancer cells** *Mol Endocrinol* **27**:266–79

18. Gebre-Medhin M., et al. (2001) **Growth hormone receptor is expressed in human breast cancer** *Am J Pathol* **158**:1217–22

19. Mertani H.C., et al. (1998) **Cellular expression of growth hormone and prolactin receptors in human breast disorders** *Int J Cancer* **79**:202–11

20. Kavarthapu R., Anbazhagan R., Dufau M.L. (2021) **Crosstalk between PRLR and EGFR/HER2 Signaling Pathways in Breast Cancer** *Cancers (Basel)* **13**

21. Wang L., et al. (2022) **Functional regulations between genetic alteration-driven genes and drug target genes acting as prognostic biomarkers in breast cancer** *Sci Rep* **12**

22. Liang J., et al. (2022) **PRLR and CACNA2D1 Impact the Prognosis of Breast Cancer by Regulating Tumor Immunity** *J Pers Med* **12**

23. Fiorillo A.A., et al. (2013) **The prolactin receptor transactivation domain is associated with steroid hormone receptor expression and malignant progression of breast cancer** *Am J Pathol* **182**:217–33

24. Schuler L.A. (2022) **Prolactin: The Third Hormone in Breast Cancer** *Front Endocrinol (Lausanne)* **13**

25. Swaminathan G., Varghese B., Fuchs S.Y. (2008) **Regulation of prolactin receptor levels and activity in breast cancer** *J Mammary Gland Biol Neoplasia* **13**:81–91

26. Hachim I.Y., et al. (2016) **Prolactin Receptor Expression is an Independent Favorable Prognostic Marker in Human Breast Cancer** *Appl Immunohistochem Mol Morphol* **24**:238–45

27. Hachim I.Y., et al. (2016) **A favorable role of prolactin in human breast cancer reveals novel pathway-based gene signatures indicative of tumor differentiation and favorable patient outcome** *Hum Pathol* **53**:142–52

28. Lopez-Ozuna V.M., et al. (2016) **Prolactin Pro-Differentiation Pathway in Triple Negative Breast Cancer: Impact on Prognosis and Potential Therapy** *Sci Rep* **6**

29. Hachim I.Y., et al. (2019) **Prolactin hormone exerts anti-tumorigenic effects in HER-2 overexpressing breast cancer cells through regulation of stemness** *Stem Cell Res* **40**

30. Agarwal N., et al. (2016) **Phase I Study of the Prolactin Receptor Antagonist LFA102 in Metastatic Breast and Castration-Resistant Prostate Cancer** *Oncologist* **21**:535–6

31. Huising M.O., Kruiswijk C.P., Flik G. (2006) **Phylogeny and evolution of class-I helical cytokines** *J Endocrinol* **189**:1–25

32. Teilum K., et al. (2005) **Solution structure of human prolactin** *J Mol Biol* **351**:810–23

33. Biener-Ramanujan E., et al. (2006) **Spatio-temporal kinetics of growth hormone receptor signaling in single cells using FRET microscopy** *Growth Hormone & Igf Research* **16**:247–257

34. Brooks A.J., et al. (2014) **Mechanism of activation of protein kinase JAK2 by the growth hormone receptor** *Science* **344**

35. Liu Y., et al. (2014) **Dynamic analysis of GH receptor conformational changes by split luciferase complementation** *Mol Endocrinol* **28**:1807–19

36. Cunningham B.C., et al. (1990) **Zinc mediation of the binding of human growth hormone to the human prolactin receptor** *Science* **250**:1709–12

37. Kossiakoff A.A., et al. (1994) **Comparison of the intermediate complexes of human growth hormone bound to the human growth hormone and prolactin receptors** *Protein Sci* **3**:1697–705

38. Fu Y.K., et al. (1992) **Growth hormone augments superoxide anion secretion of human neutrophils by binding to the prolactin receptor** *J Clin Invest* **89**:451–7

39. Somers W., et al. (1994) **The X-ray structure of a growth hormone-prolactin receptor complex** *Nature* **372**:478–81

40. Hughes J.P., Friesen H.G. (1985) **The nature and regulation of the receptors for pituitary growth hormone** *Annu Rev Physiol* **47**:469–82

41. Frank S.J. (2020) **Classical and novel GH receptor signaling pathways** *Mol Cell Endocrinol* **518**

42. Chhabra Y., et al. (2021) **GHR signalling: Receptor activation and degradation mechanisms** *Mol Cell Endocrinol* **520**

43. Herman A., et al. (2000) **Functional heterodimerization of prolactin and growth hormone receptors by ovine placental lactogen** *J Biol Chem* **275**:6295–301

44. Biener E., et al. (2003) **Ovine placental lactogen-induced heterodimerization of ovine growth hormone and prolactin receptors in living cells is demonstrated by fluorescence resonance energy transfer microscopy and leads to prolonged phosphorylation of signal transducer and activator of transcription (STAT)1 and STAT3** *Endocrinology* **144**:3532–40

45. Xu J., et al. (2011) **Growth hormone signaling in human T47D breast cancer cells: potential role for a growth hormone receptor-prolactin receptor complex** *Mol Endocrinol* **25**:597–610

46. Liu Y., et al. (2016) **GHR/PRLR Heteromultimer Is Composed of GHR Homodimers and PRLR Homodimers** *Mol Endocrinol* **30**:504–17

47. Liu Y., et al. (2017) **Subdomain 2, Not the Transmembrane Domain, Determines the Dimerization Partner of Growth Hormone Receptor and Prolactin Receptor** *Endocrinology* **158**:3235–3248

48. Huang B., Babcock H., Zhuang X. (2010) **Breaking the diffraction barrier: super-resolution imaging of cells** *Cell* **143**:1047–58

49. Bates M., Blosser T.R., Zhuang X. (2005) **Short-range spectroscopic ruler based on a single-molecule optical switch** *Phys Rev Lett* **94**

50. Kruger C.L., et al. (2017) **Quantitative single-molecule imaging of TLR4 reveals ligand-specific receptor dimerization** *Sci Signal* **10**

51. Krüger C., et al. (2017) **Molecular counting of membrane receptor subunits with single-molecule localization microscopy** *SPIE BiOS* **10071**

52. Ripley B.D. (1979) **Tests of 'Randomness' for Spatial Point Patterns** *Journal of the Royal Statistical Society. Series B (Methodological)* **41**:368–374

53. Ester M., et al. (1996) **A density-based algorithm for discovering clusters in large spatial databases with noise** *Proceedings of the Second International Conference on Knowledge Discovery and Data Mining* :226–231

54. Mattheyses A.L., Simon S.M., Rappoport J.Z. (2010) **Imaging with total internal reflection fluorescence microscopy for the cell biologist** *J Cell Sci* **123**:3621–8

55. Kohlhuber F., et al. (1997) **A JAK1/JAK2 chimera can sustain alpha and gamma interferon responses** *Mol Cell Biol* **17**:695–706

56. Loesch K., et al. (2006) **Janus kinase 2 influences growth hormone receptor metalloproteolysis** *Endocrinology* **147**:2839–49

57. Deng L., et al. (2007) **Determinants of growth hormone receptor down-regulation** *Mol Endocrinol* **21**:1537–51

58. Zhang Y., et al. (2019) **Growth hormone (GH) receptor (GHR)-specific inhibition of GH-Induced signaling by soluble IGF-1 receptor (sol IGF-1R)** *Mol Cell Endocrinol* **492**

59. Jiang J., et al. (1998) **Growth hormone-dependent tyrosine phosphorylation of a GH receptor-associated high molecular WEIGHT protein immunologically related to JAK2** *Biochem Biophys Res Commun* **253**:774–9

60. Jiang J., et al. (2004) **A conformationally sensitive GHR [growth hormone (GH) receptor] antibody: impact on GH signaling and GHR proteolysis** *Mol Endocrinol* **18**:2981–96

61. Beggs R.R., Dean W.F., Mattheyses A.L. (2020) **dSTORM Imaging and Analysis of Desmosome Architecture** *Methods Mol Biol*

62. Beggs R.R., et al. (2022) **Desmosomes undergo dynamic architectural changes during assembly and maturation** *Tissue Barriers* **10**

63. Pageon S.V., et al. (2016) **Clus-DoC: a combined cluster detection and colocalization analysis for single-molecule localization microscopy data** *Mol Biol Cell* **27**:3627–3636

64. Frank S.J. (2002) **Receptor dimerization in GH and erythropoietin action--it takes two to tango, but how?** *Endocrinology* **143**:2–10

65. Cunningham B.C., et al. (1991) **Dimerization of the extracellular domain of the human growth hormone receptor by a single hormone molecule** *Science* **254**:821–5

66. Gent J., et al. (2002) **Ligand-independent growth hormone receptor dimerization occurs in the endoplasmic reticulum and is required for ubiquitin system-dependent endocytosis** *Proc Natl Acad Sci U S A* **99**:9858–63

67. Gadd S.L., Clevenger C.V. (2006) **Ligand-independent dimerization of the human prolactin receptor isoforms: functional implications** *Mol Endocrinol* **20**:2734–46

68. Wilmes S., et al. (2020) **Mechanism of homodimeric cytokine receptor activation and dysregulation by oncogenic mutations** *Science* **367**:643–652

69. Pezet A., et al. (1997) **The last proline of Box 1 is essential for association with JAK2 and functional activation of the prolactin receptor** *Mol Cell Endocrinol* **129**:199–208

70. Kassem N., et al. (2021) **Order and disorder-An integrative structure of the full-length human growth hormone receptor** *Sci Adv* **7**

71. Bugge K., et al. (2016) **A combined computational and structural model of the full-length human prolactin receptor** *Nat Commun* **7**

72. Ferrao R.D., Wallweber H.J., Lupardus P.J. (2018) **Receptor-mediated dimerization of JAK2 FERM domains is required for JAK2 activation** *Elife* **7**

Article and author information

Chen Chen
Department of Genetics, University of Alabama at Birmingham, Birmingham, USA, Division of Endocrinology, Diabetes, and Metabolism, Department of Medicine, University of Alabama at Birmingham, Birmingham, USA

Jing Jiang
Division of Endocrinology, Diabetes, and Metabolism, Department of Medicine, University of Alabama at Birmingham, Birmingham, USA

Tejeshwar C. Rao
Department of Cell, Developmental, and Integrative Biology, University of Alabama at Birmingham, Birmingham, USA

Tatiana T. Marquez Lago
Department of Genetics, University of Alabama at Birmingham, Birmingham, USA

Stuart J. Frank
Division of Endocrinology, Diabetes, and Metabolism, Department of Medicine, University of Alabama at Birmingham, Birmingham, USA
For correspondence: sjfrank@uab.edu
ORCID iD: 0000-0001-7768-623X

André Leier
Department of Genetics, University of Alabama at Birmingham, Birmingham, USA
For correspondence: leier@uab.edu
ORCID iD: 0000-0002-2647-2693

Copyright

Editors

Reviewer #1 (Public Review):

In this study, Chen et al. used super-resolution microscopy on T47D cells to investigate the cell surface distribution of hGHR and hPRLR in steady-state and in response to ligand stimulation. The initial findings of this study suggest both PRL and GH stimulation lead to a decrease in GH receptors but an increase in the PRLR on the cell surface. A subset of both receptors co-localize in close proximity and may form heteromers. Moreover, the study revealed that the box 1 region in GHR plays an essential role in the regulation of its interaction with the PRLR, and the box 1 region in the PRLR is involved in the PRL-induced downregulation of the GHR. The most innovative aspect of this study is the super-resolution microscopy methodology that permits the analysis of proteins on the level of single molecules, and other notable advances are the generation of T47D cells that lack the PRLR and GHR. The questions after reading this manuscript are what novel insights have been gained that significantly go beyond what was already known about the interaction of these receptors and, more importantly, what are the physiological implications of these findings? The proposed significance of the results in the last paragraph of the Discussion section is speculative since none of the receptor interactions have been investigated in TNBC cell lines. Moreover, no physiological experiments were conducted using the PRLR and GH knockout T47D cells to provide biological relevance for the receptor heteromers. The proposed role of JAK2 in the cell surface distribution and association of both receptors as stated in the title was only derived from the analysis of box 1 domain receptor mutants. A knockout of JAK2 was not conducted to assess heteromer formation.

There are additional points that require the authors' attention:

1. Except for some investigation of γ2A-JAK2 cells, most of the experiments in this study were conducted on a single breast cancer cell line. In terms of rigor and reproducibility, this is somewhat borderline. The CRISPR/Cas9 mutant T47D cells were not used for rescue experiments with the corresponding full-length receptors and the box1 mutants. A missed opportunity is the lack of an investigation correlating the number of receptors with physiological changes upon ligand stimulation (e.g., cellular clustering, proliferation, downstream signaling strength).

2. An obvious shortcoming of the study that was not discussed seems to be that the main methodology used in this study (super-resolution microscopy) does not distinguish the presence of various isoforms of the PRLR on the cell surface. Is it possible that the ligand stimulation changes the ratio between different isoforms? Which isoforms besides the long form may be involved in heteromer formation, presumably all that can bind JAK2?

3. Changes in the ligand-inducible activation of JAK2 and STAT5 were not investigated in the T47D knockout models for the PRL and GHR. It is also a missed opportunity to use super-resolution microscopy as a validation tool for the knockouts on the single cell level and how it might affect the distribution of the corresponding other receptor that is still expressed.

4. Why does the binding of PRL not cause a similar decrease (internalization and downregulation) of the PRLR, and instead, an increase in cell surface localization? This seems to be contrary to previous observations in MCF-7 cells (J Biol Chem. 2005 October 7; 280(40): 33909-33916).

5. Some figures and illustrations are of poor quality and were put together without paying attention to detail. For example, in Fig 5A, the GHR was cut off, possibly to omit other nonspecific bands, the WB images look 'washed out'. 5B, 5D: the labels are not in one line over the bars, and what is the point of showing all individual data points when the bar graphs with all annotations and SD lines are disappearing? As done for the y2A cells, the illustrations in 5B-5E should indicate what cell lines were used. No loading controls in Fig 5F, is there any protein in the first lane? No loading controls in Fig 6B and 6H.

6. The proximity ligation method was not described in the M&M section of the manuscript.

Reviewer #2 (Public Review):

Summary:
Chen Chen et al. investigated the interaction between GHR and PRLR at the cell surface using STORM-type super-resolution microscopy, proximity ligation assay, and mutagenesis. They found that GH and PRL change the surface expression of GHR and PRLR. Upon stimulation, the hGHR cluster size significantly increases in a transient manner, whereas changes in hPRLR occur more slowly. In their previous publication, the authors found that hGHR and hPRLR co-immunoprecipitate in the absence of ligands. Based on that finding and the observations here, the authors examined colocalization of hGHR and hPRLR in clusters with proximity ligation assays and found that the receptors form complexes on the surface of T47D cells, and that these complexes respond differently to the ligands. Remarkably, the experiments in cells lacking either hGHR or hPRLR showed that PRLR is necessary for the reduction of surface hGHR induced by PRL. Studies with truncation or deletion of hPRLR mutants, suggest the box 1 region in hPRLR plays a critical role in stabilizing the hGHR-hPRLR complexes. This region contains the JAK2 binding site, and the authors show that binding of JAK2 to hGHR is also required for hPRLR-mediated regulation of hGHR surface expression. Cytokine receptors have very important broad-ranging roles in regulating cells and physiological roles. Therefore, the new findings described here will significantly expand our understanding of the structure-function relationship that drives a core signalling mechanism in cell biology.

Strengths:
I particularly appreciate that the authors used different angles to examine the mechanism of GHR-PRLR interaction and that they also checked the conclusions with CRISPR/Cas9 technology and with a cellular reconstitution system.

Weaknesses:
I could not fully evaluate some of the data, mainly because several details on acquisition and analysis are lacking. It would be useful to know what the background signal was in dSTORM and how the authors distinguished the specific signal from unspecific background fluorescence, which can be quite prominent in these experiments. Typically, one would evaluate the signal coming from antibodies randomly bound to a substrate around the cells to determine the switching properties of the dyes in their buffer and the average number of localisations representing one antibody. This would help evaluate if GHR or PRLR appeared as monomers or multimers in the plasma membrane before stimulation, which is currently a matter of debate. It would also provide better support for the model proposed in Figure 8. Since many of the findings in this work come from the evaluation of localisation clusters, an image showing actual localisations would help support the main conclusions. I believe that the dSTORM images in Figures 1 and 2 are density maps, although this was not explicitly

stated. Alexa 568 and Alexa 647 typically give a very different number of localisations, and this is also dependent on the concentration of BME. Did the authors take that into account when interpreting the results and creating the model in Figures 2 and 8? I believe that including this information is important as findings in this paper heavily rely on the number of localisations detected under different conditions. Including information on proximity labelling and CRISPR/Cas9 in the methods section would help with the reproducibility of these findings by other groups.

Reviewer #3 (Public Review):

Summary:
The authors are interested in the relative importance of PRL versus GH and their interactive signaling in breast cancer. After examining GHR-PRLR interactions in response to ligands, they suggest that a reduction in cell surface GHR in response to PRL may be a mechanism whereby PRL can sometimes be protective against breast cancer.

Strengths:
The strengths of the study include the interesting question being addressed and the application of multiple complementary techniques, including dSTORM, which is technically very challenging, especially when using double labeling. Thus, dSTORM is used to show co-clustering of GHR and PRLR, and, in response to PRL, rapid internalization of GHR and increased cell surface PRLR. Proximity ligation assays demonstrate that some GHR and PRLR are within 40 nm (≈ 4 plasma membranes) of each other and that upon ligand stimulation, they move apart. Intact receptor knockin and knockout approaches and receptor constructs without the Jak2 binding domain demonstrate a) a requirement for the PRLR for there to be PRL-driven internalization of GHR, and b) that Jak2-PRLR interactions are necessary for the stability of the GHR-PRLR colocalizations.

Weaknesses:
The manuscript suffers from a lack of detail, which in places makes it difficult to evaluate the data and would make it very difficult for the results to be replicated by others. In addition, the manuscript would very much benefit from a full discussion of the limitations of the study. For example, the manuscript is written as if there is only one form of the PRLR while the anti-PRLR antibody used for dSTORM would also recognize the intermediate form and short forms 1a and 1b on the T47D cells. Given the very different roles of these other PRLR forms in breast cancer (Dufau, Vonderhaar, Clevenger, Walker and other labs), this limitation should at the very least be discussed. Similarly, the manuscript is written as if Jak2 essentially only signals through STAT5 but Jak2 is involved in multiple other signaling pathways from the multiple PRLRs, including the long form. Also, while there are papers suggesting that PRL can be protective in breast cancer, the majority of publications in this area find that PRL promotes breast cancer. How then would the authors interpret the effect of PRL on GHR in light of all those non-protective results?